A global off-line model of size-resolved aerosol microphysics: II. Identification of key uncertainties

D. V. Spracklen, K. J. Pringle, K. S. Carslaw, M. P. Chipperfield, G. W. Mann

Atmos. Chem. Phys. Discuss., 5, 3437–3489, 2005
www.atmos-chem-phys.org/acpd/5/3437/
SRef-ID: 1680-7375/acpd/2005-5-3437
European Geosciences Union

Atmospheric Chemistry and Physics Discussions

A global off-line model of size-resolved aerosol microphysics: II. Identification of key uncertainties

D. V. Spracklen, K. J. Pringle, K. S. Carslaw, M. P. Chipperfield, and G. W. Mann

Institute of Atmospheric Science, School of Earth and Environment, University of Leeds, UK

Received: 21 January 2005 – Accepted: 16 April 2005 – Published: 30 May 2005

Correspondence to: D. V. Spracklen (dominick@env.leeds.ac.uk)

Abstract

We use the new GLOMAP model of global aerosol microphysics to investigate the sensitivity of modelled sulfate and sea salt aerosol properties to uncertainties in the driving microphysical processes and compare these uncertainties with those associated with aerosol and precursor gas emissions. Overall, we conclude that uncertainties in microphysical processes have a larger effect on global condensation nuclei (CN) and cloud condensation nuclei (CCN) concentrations than uncertainties in present-day sulfur emissions. Our simulations suggest that uncertainties in predicted sulfate and sea salt CCN abundances due to poorly constrained microphysical processes are likely to be of a similar magnitude to long-term changes in CCN due to changes in anthropogenic emissions. A microphysical treatment of the global sulfate aerosol allows the uncertainty in climate-relevant aerosol properties to be attributed to specific processes in a way that has not been possible with simpler aerosol schemes. In particular we conclude that: (1) changes in the binary H_2SO_4-H_2O nucleation rate and condensation rate of gaseous H_2SO_4 cause a shift in the vertical location of the upper tropospheric CN layer by as much as 3 km, while changes in absolute concentration are relatively small; (2) uncertainties in the binary H_2SO_4-H_2O nucleation rate have a relatively insignificant effect on boundary layer aerosol properties; (3) production of sulfate particles in power plant plumes below the scale of the model grid (which is of the order of 300 km) has the potential to change the global mean sulfate-derived CN concentration by a factor 2 or more at the surface, and changes of up to a factor 20 can occur in polluted regions; (4) predicted global mean sulfate and sea salt CCN concentrations change by 10 to 40% at the surface when several microphysical processes are changed within reasonable uncertainty ranges; (5) CCN concentrations are particularly sensitive to primary sulfate particle emissions, with global mean CCN changing by up to 40% and local concentrations changing by more than 100% when the percentage of anthropogenic SO_2 emitted as particulates in plumes is changed from 0 to 5%; (6) uncertainties in CCN due to the mode of sulfate emission (i.e., the fraction of sulfur emitted as primary particles) are

ACPD

5, 3437–3489, 2005

larger than those (∼15%) caused by a ±25% change in total sulfur emissions; (7) large changes in sea spray flux have insignificant effects on global sulfate aerosol except when the mass accommodation coefficient of sulfuric acid on the salt particles is set unrealistically low.

1. Introduction

Several global aerosol models have recently been developed that include a full size-resolved (sectional) treatment of the aerosol mass and number (Gong et al., 1997, 2003; Jacobson, 2001; Adams and Seinfeld, 2002, 2003; Spracklen et al., 2005). Although global simulations with these models have mostly been restricted to just sea salt (Gong et al., 1997), sulfate (Adams and Seinfeld, 2002) or their combination (Adams and Seinfeld, 2003; Gong et al., 2003; Spracklen et al., 2005), much has been learned about the factors that control the aerosol size distribution in different atmospheric regions. These global sectional aerosol models calculate aerosol properties from first principles without making assumptions about the shape of the size distribution. Once these models have been evaluated against modern observations they should be useful tools for calculating global CCN concentrations without the need for simple parameterisations relating aerosol mass or number to CCN number. This is an important development as a better estimation of the anthropogenic effects on CCN number is essential for quantification of the aerosol indirect effect.

An essential part of the development of these models is to quantify the robustness of the predicted aerosol size distribution, given quite large uncertainties in microphysical processes and emissions. This paper is the second of three papers describing a new GLObal Model of Aerosol Processes (GLOMAP). The first paper described the model and the global simulation of sulfate and sea salt aerosol properties (Spracklen et al., 2005). This second paper examines the sensitivity of the predicted aerosol size and spatial distribution to uncertainties in the microphysical processes that control these two aerosol types. The third paper will present a detailed comparison of the model

against aerosol observations.

Sensitivity studies of direct radiative forcing have generally shown a weak dependence on the assumed aerosol size distribution (Kiehl and Briegleb, 1993; Boucher and Anderson, 1995; Nemesure et al., 1995; Pilinis et al., 1995; Pan et al., 1997). In contrast to these earlier studies, Myhre et al. (2004) showed that relatively small changes in size distribution can change the direct radiative forcing by up to 15%. Sensitivity studies of indirect radiative forcing by sulfate aerosols show that uncertainty in the shape of the aerosol distribution is one of the largest contributors to model uncertainty (Pan et al., 1998), indicating that size-resolved global aerosol models are required for an accurate description of indirect radiative forcing.

Aerosol box models have been used to understand the processes controlling aerosol properties in the remote marine boundary layer (MBL) (Pandis et al., 1994; Raes, 1995; Kerminen and Wexler, 1997; Capaldo et al., 1999; Yoon and Brimblecombe, 2002). Raes (1995) showed that the sensitivity of MBL number concentration to the accommodation coefficient and nucleation rate was small compared to the sensitivity to environmental variables such as the rate of entrainment of aerosol from the free troposphere (FT). For example, both Raes (1995) and Capaldo et al. (1999) showed that entrainment of FT aerosol into the MBL could suppress MBL aerosol nucleation. However, Capaldo et al. (1999) also showed that modelled MBL aerosol number depended sensitively on the H_2SO_4 accommodation coefficient, nucleation rate and washout efficiency.

Adams and Seinfeld (2002) used a global aerosol model to show that both CN and CCN concentrations are sensitive to changes in the assumed nucleation rate and to primary particulate emissions from anthropogenic sulfur emissions. Here, we use GLOMAP to explore the sensitivity to a much larger range of microphysical processes affecting sulfate and sea salt aerosol and compare the resulting changes in CN and CCN with those due to uncertainties in emissions of both sulfur species and sea spray.

2. Model Description

GLOMAP is an extension to the TOMCAT global 3-D off-line chemical transport model (CTM) (Stockwell and Chipperfield, 1999). GLOMAP includes the processes of aerosol nucleation, condensation, growth, coagulation, wet and dry deposition, transport, and cloud processing. A full description of GLOMAP is given in Spracklen et al. (2005). The aerosol distribution is described using a sectional scheme with 20 bins spanning dry diameters from about 1 nm to 25 μm. Two moments are simulated in each section (number density and mass per particle). GLOMAP, as used here, is currently restricted to sea salt and sulfate aerosol.

Spracklen et al. (2005) showed that GLOMAP is capable of simulating realistic MBL CN and CCN concentrations under conditions where sulfate and sea salt are the dominant components of the aerosol. In the MBL the model simulates the submicron bimodal distribution with Aitken mode and accumulation mode simulated at approximately the correct sizes. In the lower FT the model simulates a unimodal distribution.

In this study we use a spatial resolution of 2.8°×2.8° latitude × longitude with 31 hybrid σ-p levels extending from the surface to 10 hPa. In the experiments performed here large-scale atmospheric transport is specified from European Centre for Medium-Range Weather Forecasts (ECMWF) analyses at 6-hourly intervals. The model was initialised with an aerosol-free atmosphere (on 1 October, 1995) and spun up for 45 days before sensitivity studies were started.

CN are defined as particles larger than 3 nm diameter. This size corresponds to the detection limit of current instrumentation (Stolzenburg and McMurry, 1991; McMurry, 2000). CCN concentrations are calculated at 0.2% supersaturation which is typical of marine stratocumulus clouds, and corresponds to the activation of particles having a dry diameter of about 70 nm. All aerosol concentrations are quoted at standard temperature and pressure (STP, 273 K and 1 atm).

ACPD
5, 3437–3489, 2005

3. Limitations of this study

In this paper we restrict our analysis of microphysical uncertainties to sulfate and sea salt aerosols, which is the simplest aerosol system involving primary and secondary particles. We take this approach primarily because sensitivity studies have a high computational cost, but also because sulfate aerosols have been the most studied aerosol type in previous climate model simulations. In these earlier simulations, sulfate aerosol was sometimes the only aerosol type included or it was simulated alongside other aerosol types such as black carbon, dust and, more recently, organic carbon (IPCC, 2001). However, until very recently, the different aerosol types were treated as non-interacting. Our simulations, while more complete in their treatment of microphysical processes, also implicitly assume that sulfate and sea salt aerosol can be treated as being independent of other aerosol types. We stress that our conclusions regarding the sensitivity of CN and CCN concentrations to uncertain microphysical parameters apply to a subset of the total atmospheric aerosol.

4. The effect of different microphysical processes

Figure 1 shows how different microphysical processes influence the modelled size distribution in the North Atlantic MBL. The effect of each process in shaping the distribution has been examined by removing one microphysical process at a time. Individual microphysical processes were switched off for 8 days and then the simulated distribution compared to the baseline distribution where all processes were included.

Without aqueous phase processing the separate accumulation mode and Aitken mode in the MBL distribution disappear, being replaced by one broad sub-micrometer mode similar to that simulated in the free troposphere. This modelled effect supports the idea that aqueous phase oxidation of SO_2 is responsible for the MBL sub-micrometer bimodal distribution (Hoppel et al., 1986).

Without coagulation there is a large increase in the number of small particles and

ACPD
5, 3437–3489, 2005

the mean diameter of the Aitken mode is shifted to smaller sizes. Coagulation removes small particles (which have high mobility and high rates of diffusion so they coagulate rapidly) but has little influence on larger particles (that have slower rates of diffusion).

Condensation of H_2SO_4 onto the existing particles reduces the concentration of gas phase H_2SO_4. With condensation switched off gas phase H_2SO_4 concentrations build up and additional nucleation occurs. This causes an increase in the concentration of small particles in the MBL and a reduction in the size of the Aitken mode. Additionally, the concentration of accumulation mode particles is reduced while their mean diameter is increased. Lack of condensational growth means fewer particles reach the diameter required for activation into cloud droplets. Fewer particles add mass though in-cloud oxidation resulting in the lower accumulation mode number. However, in-cloud oxidation is often H_2O_2 limited and so when fewer particles are activated these particles may grow to larger sizes.

Switching off particle wet removal processes causes an increase in the concentration of aerosols larger than about 100 nm diameter. In particular, the number of particles in the accumulation mode is greatly increased. This has the effect of increasing the surface area of the aerosol distribution. This increased surface area causes greater condensation of gaseous H_2SO_4 onto the particle distribution and less new particle formation. The number of small particles (with dry diameter less than about 40 nm) is lower without wet removal processes.

Switching off sea spray emissions causes a large reduction in the number of particles larger than about 200 nm dry diameter. This demonstrates in a simple way the division between particles comprised mainly of sulfate and those comprised mainly of sea spray. The size distribution of particles smaller than 200 nm is virtually unchanged. Switching off sea salt emissions reduces particle surface area in the MBL but has little effect on surface area in the UT, which is where binary H_2SO_4–H_2O nucleation predominately occurs in our model (in contrast to the effect of wet scavenging, which affects particle surface areas right through the FT). Nucleation rates are therefore not greatly affected and the number of particles entraining from the UT is virtually unchanged.

This effect is studied in greater detail in Sect. 5.6 where the model sensitivity to the emission strength of sea spray is explored.

Switching off dry deposition causes an increase in the number of simulated particles throughout the aerosol size distribution. Dry deposition occurs only at the surface and as for changes in sea spray emissions only changes surface area in the MBL and not in the UT where new particle production occurs. Therefore, switching off dry deposition does not cause the reduction in new UT particle formation and the decrease in MBL Aitken mode particle that is observed for wet deposition.

5. The effect on global aerosol of uncertainties in microphysics and emissions

It is important to understand how robust the simulated aerosol properties are, given often quite large uncertainties in the rates of microphysical processes. In this section we examine the effect of uncertainties in the sulfuric acid aerosol nucleation rate, the condensation rate of gaseous H_2SO_4 and the size of the nucleation cluster. We also examine the effect of changing the activation radius for cloud drop formation for aqueous SO_2 oxidation and in-cloud nucleation scavenging. The effects of these microphysical uncertainties are then compared with the effects of uncertainties in the emission rates of sulfur species and of sea spray particles.

To perform these sensitivity studies two global aerosol fields were compared. In the first run, the global aerosol field was calculated over a 90-day period (including a spin-up from an aerosol-free atmosphere). In the second run, the model was spun up for a period of 45 days, then a particular processes were changed and the model was run for a further 45 days. Aerosol properties in these two runs are compared for the last 30 days of the 90-day model runs. Comparisons with model runs over longer time periods showed that this length of model run is sufficient to capture most of the change that occurred due to changes in parameterisation rates.

5.1. Sensitivity to nucleation and condensation rates

Accurately including a description of particle nucleation in a global model is difficult. There are significant uncertainties in the rate of nucleation and even the mechanisms that predominate in the atmosphere (e.g., Kulmala et al. (2004)). Binary H_2SO_4–H_2O nucleation has been the most studied mechanism, but there are examples where this mechanism seems unable to explain observed nucleation events (Weber et al., 1995; Kulmala et al., 2004). NH_3 lowers the vapour pressure of H_2SO_4 above solution surfaces (Marti et al., 1997), and may increase nucleation rates by several orders of magnitude (Coffman and Hegg (1995); Napari et al. (2002)). Particle nucleation rates are strong nonlinear functions of temperature and precursor gas vapour pressure. Therefore sub-grid scale variations in humidity, temperature or H_2SO_4 concentration could lead to higher nucleation rates than the mean conditions would suggest. Sub-grid scale variability may occur through atmospheric mixing, waves, turbulence, convective eddies or cloud outflow (Easter and Peters, 1994; Nilsson et al., 2000; Clarke et al., 1998).

The binary H_2SO_4–H_2O homogeneous nucleation rate, which we use here (Spracklen et al., 2005), is uncertain to within several orders of magnitude even under conditions where laboratory measurements are available (Vehkamäki et al., 2002). The most recent paramaterisations (Vehkamäki et al., 2002), while more physically realistic, do not agree better with the limited laboratory measurements than earlier simpler schemes (Kulmala et al., 1998). Nucleation rates below the temperature limit of observations (236 K) may be even less reliable. Other nucleation mechanisms are also clearly involved in the atmosphere (Kulmala et al., 2004). Sensitivity studies involving nucleation rates are therefore likely to be fairly conservative. In this work, we use the nucleation parameterisation of Kulmala et al. (1998), which is valid down to 233 K. Below this temperature we use the rate at 233 K. Figure 2 shows how the rate we use depends on temperature and humidity for a fixed realistic gas phase H_2SO_4 concentration of 3×10^7 cm^{-3}. Our sensitivity studies then explore how important vari-

ations in the rate of nucleation are likely to be for aerosol distributions. Such sensitivity tests provide a reasonable measure of how the global aerosol depends on the binary homogeneous nucleation rate and suggest what improvement in parameterised rates is needed.

5.1.1. Balance of nucleation and condensation

Nucleation of new sulfuric acid particles and condensation of H_2SO_4 onto existing particles compete for available gas phase H_2SO_4. This competition means that uncertainties in the rates of both processes will affect the atmospheric concentration of CN. We therefore examine the effect of uncertainties in both processes together. The results are shown in Figs. 3 and 4. GLOMAP attempts to capture the competition between nucleation and condensation by selecting a short timestep (generally about 90 s) over which these processes are calculated (Spracklen et al., 2005).

Nucleation rates (j) were changed by varying the H_2SO_4 nucleation threshold (the H_2SO_4 concentration at which a nucleation rate of 1 cm^{-3} s^{-1} is calculated) in the Kulmala et al. (1998) parametrisation. A doubling or halving of the nucleation threshold causes approximately a factor 10 change in j (Fig. 2).

Condensation rates were changed by changing the accommodation coefficient, a_e, which defines the probability that a molecule of H_2SO_4 will become bound to a particle upon collision. There is considerable uncertainty in the magnitude of a_e. Van Dingenen and Raes (1991) report values of a_e in the range of 0.02 to 0.1. The theoretical studies of Clement et al. (1996) and the field measurements of Weber et al. (1995) report values of a_e close to unity. Poschl et al. (1998) experimentally determined a_e at 303 K with a lower limit of 0.43 and a best fit value of 0.65. Jefferson et al. (1997) measured H_2SO_4 uptake onto $(NH_4)_2SO_4$ aerosol and reported values of 0.73±0.21 and onto NaCl aerosol of 0.79±0.23. Pandis et al. (1994) and Russell et al. (1994) used a value of 0.02; Raes (1995), 0.3; Katoshevski et al. (1999), 1.0; Adams and Seinfeld (2002), 0.65 and Easter et al. (2004), 0.02. Laboratory and field studies have shown that the value of a_e is reduced as a particle becomes increasingly covered in surfactants

(Däumer et al., 1992). Marine air contains substantial surfactant concentrations from ocean bubble bursting which may be able to coat marine aerosol particles, thereby reducing accommodation coefficients.

Figures 3 and 4 show that increasing j (or decreasing a_e) causes an increase in CN concentrations below about 200–400 hPa and a decrease in CN at higher levels. In the upper troposphere the pattern of response to increasing j or decreasing a_e is similar, with changes >50%. These fractional changes in CN concentration appear to be counterintuitive as one might expect an increase in CN concentration in response to an increased nucleation rate. Figure 5 shows altitude profiles for a remote marine situation and a polluted continental situation and gives a rather different perspective on how CN concentrations change. In both locations, changing j and a_e changes the altitude in the UT at which the maximum CN concentration occurs (a shift of about 1.5 km for a factor 10 change in j or 3 km for a change in a_e from 1.0 to 0.3), while the shape of the CN profile is essentially preserved. Increasing j (or decreasing a_e) decreases the altitude of the CN maximum, whereas decreasing j (or increasing a_e) increases the altitude of the CN maximum. This shift in altitude of the CN layer has important consequences for comparing model CN number against UT CN measurements. Comparisons with measurements would look poor even if the model captured the shape and magnitude of the CN maximum correctly but simulated a 1–2 km error in the altitude of the maximum.

Figure 5 also shows changes in the vertical profile of the total particle concentration (including particles smaller than 3 nm diameter). These look very different from the changes in CN, with increasing nucleation rates now causing increases in the total particle concentration and no change in the altitude at which the maximum concentration occurs. Reducing the H_2SO_4 nucleation threshold increases the rate of production of nucleation clusters, which, at any altitude, gives rise to higher concentrations of nucleation clusters and hence also total aerosol. The concentration of CN depends on the number of nucleation clusters that survive coagulational scavenging up to 3 nm diameter. The number of CN therefore depends on the competition between nucleation

and condensation for available H_2SO_4. As altitude increases, temperature decreases causing the H_2SO_4 nucleation threshold to decrease. Thus at higher altitudes the gas phase H_2SO_4 concentrations, and hence condensation rates, tend to be lower, which reduces cluster growth rates and increases the fraction of clusters that are coagulationally scavenged before reaching 3 nm. The altitude of the CN maximum occurs where the combination of the nucleation and condensation rates gives rise to the highest CN number. As j increases (or a_e decreases) the altitude at which this occurs decreases causing the decrease in the altitude of the CN maximum.

Below the UT the response of CN concentrations to changes in j and a_e depends on the abundance of sulphur species. Over polluted regions (Figs. 5b and d) CN concentrations in the lower atmosphere change by more than a factor of 2 when j and a_e are changed. In polluted continental regions, where more gas phase H_2SO_4 is present, particle growth rates are faster and increased nucleation rates leads to higher BL number concentrations as more nucleation mode particles grow fast enough to survive coagulational scavenging. The effect of changes in a_e is particularly marked in the polluted lower troposphere (Fig. 5d), where CN concentrations increase by up to a factor of 20 when a_e is reduced from 1.0 to 0.02. Reducing a_e this much allows BL gas phase H_2SO_4 concentrations to build up sufficiently to allow BL binary H_2SO_4–H_2O nucleation to occur. In contrast, tropical remote MBL locations (Figs. 5a and c) typically show less than a 10% change in CN concentrations when j changes by an order of magnitude. In such clean locations the low H_2SO_4 concentrations ensure that nucleation occurs almost exclusively in the UT.

Below the UT, the response of CN to changes in j and a_e is also dependent on the temperature. Low FT temperatures allow nucleation to occur nearer the surface. Figure 6 shows that changes in CN in the Southern Ocean BL (40°–60° S) are in excess of 100% when j changes by a factor 10, but are considerably less in the tropics.

Changing nucleation rates by an order of magnitude causes about a 5–8% change in global mean CCN concentrations. Reducing the accommodation coefficient from 1.0 to 0.3 causes little effect on global mean CCN concentrations. However, reducing

condensation rates further (by reducing a_e to 0.02) causes about a 20% reduction in global CCN concentrations.

Conclusions regarding the sensitivity of CN and CCN concentrations to changes in nucleation and condensation rates are of course restricted to simulations using a binary H_2SO_4–H_2O homogeneous nucleation rate. The scheme we use produces particles mostly in the cold UT and FT. Changes in BL CN therefore tend to be rather small. Observations suggest that CN can also be produced in the planetary boundary layer (Kulmala et al., 2004), perhaps assisted by condensation of organic vapours. It is therefore likely that these simulations underpredict the effect that changes in nucleation rate have on the BL aerosol distribution.

5.1.2. Sensitivity to the nucleation cluster size

The nucleation critical cluster is the smallest size above which a cluster of H_2SO_4 molecules is stable. The nucleation parametrisation of Kulmala et al. (1998) does not provide any information on the critical cluster size of the nucleating particles, although more recent parametrisations do (Vehkamäki et al., 2002). The sensitivity to the cluster size was investigated by reducing the cluster size from 100 to 10 molecules of H_2SO_4.

Reducing the critical cluster size causes a downward shift in the altitude of the CN maximum (by as much as 3 km) and an overall reduction in the concentration (Fig. 7). However, altitude profiles of total particle number (including particles less than 3 nm diameter) have the same shape irrespective of the critical cluster size, with smaller critical clusters giving greater particle number at any altitude in the UT.

Smaller critical clusters take longer to grow to observable sizes (>3 nm diameter) where they are counted as CN. Smaller clusters are therefore subject to coagulational scavenging for a longer period of time, which causes a reduction in CN concentration (smaller particles also have higher mobility and therefore higher coagulational loss rates). The shift in altitude of the CN maximum can be explained by changes in the growth and coagulation rates with altitude for different initial cluster sizes: smaller critical clusters take longer to grow to CN sizes and are more likely to be coagulation

scavenged. As altitude increases, the temperature falls and gives rise to a reduced H_2SO_4 nucleation threshold. This causes reduced gas phase H_2SO_4 concentrations which in turn causes reduced condensational growth rates. Rates of coagulational scavenging are fairly stable with altitude (due to relatively stable Aitken mode concentrations) which means as altitude increases nucleation clusters are more likely to be scavenged before they can grow into CN sized particles. Therefore as the critical cluster size is decreased the altitude at which nucleation clusters will be more likely to grow into CN than be scavenged also decreases.

Global mean surface CN concentrations change by less than 5%. Global mean CCN concentrations (not shown) are virtually unaffected, changing by less than 1%.

5.2. Sensitivity to aqueous phase oxidation

In GLOMAP, aerosol particles are assumed to activate into cloud droplets when low cloud is present and the particle diameter is greater than a preset fixed diameter. In the baseline model runs, aerosol particles are assumed to activate at an equivalent dry diameter of 0.05 μm. Figure 8 shows the sensitivity of simulated aerosol distributions to a change in this activation diameter.

The changes in CCN concentration shown in Fig. 8 are calculated at 0.2% supersaturation. The activation diameter used during the model simulation was fixed at 0.05 μm in the baseline run and 0.08 μm (corresponding to 0.18% supersaturation) in the sensitivity run. In the atmosphere the activation diameter will vary greatly from one cloud to another and from region to region driven partly by variations in updraught velocity. Effectively, we are simulating repeated aerosol activation and aqueous processing at a fixed high or low supersaturation and then examining the effect of such events on the CCN abundance at some average supersaturation of 0.2%.

Increasing the activation diameter from 0.05 to 0.08 μm reduces global mean CCN number at 0.2% supersaturation by around 30%. Using a smaller activation diameter in the model allows a greater proportion of the particles to grow rapidly through aqueous phase oxidation of SO_2 while the particles exist as cloud droplets. This growth of small

particles leads to a greater concentration of particles that can be activated at more moderate supersaturations of 0.2%.

Figure 9a shows how a change in the activation diameter affects the simulated number-size distribution in the subtropical MBL. Changes in the size distribution are apparent between 10 nm and about 1 μm. Above about 1 μm the number-size distribution is dominated by sea salt emission and deposition fluxes. Increasing the size of the activation diameter for cloud processing causes an increase in the mean diameter of the Aitken mode from ~25 nm to around ~60 nm. Increasing the activation diameter also reduces the number and increases the mean diameter of the accumulation mode. In many cases aqueous phase oxidation will be H_2O_2 limited. At larger activation diameters the fewer particles that are large enough to activate will share the available H_2O_2. These fewer activated particles will therefore tend to add more mass and grow to larger sizes.

These results can also be shown as a change in the CCN spectrum. Measurements made using CCN counters give the number concentration of CCN active at particular supersaturations (Gras, 1995; Ayers and Gillett, 2000). Figure 9b shows the simulated CCN number concentration at supersaturations between 0 and 1% for the 4 model runs with different particle activation diameters. The CCN number concentration is calculated for each supersaturation using Kohler theory, assuming that particles larger than the critical diameter instantly grow into cloud droplets. As the supersaturation is increased from 0 to 1% the number concentration of activated particles increases as the diameter of activation decreases. At very low supersaturations only large sea salt particles will activate and the number of CCN are identical for all the different activation diameters. At slightly higher supersaturations (0.01–0.04%) larger activation diameters result in greater CCN number due to the larger mean size of the simulated accumulation mode. At slightly higher supersaturations (between about 0.06 and 0.4%) the number of CCN is greater for smaller model activation diameters. Smaller activation diameters mean that a greater subset of the particle population in activated and adds mass through aqueous-phase oxidation. However, as the supersaturation is raised

further (to 0.4–1%) the CCN concentrations are slightly larger for small activation diameters. Smaller activations diameters give an increase in the mean diameter of the simulated Aitken mode, which are then activated as the supersaturation increases.

Finally, it is worth noting that changing the diameter of activation has little effect on global mean CN concentrations, which change by about 1–2% when the diameter of activation changes from 0.04 to 0.08 μm.

5.3. Sensitivity to nucleation scavenging

Loss of aerosol due to nucleation, or in-cloud, scavenging is a complex process that can be viewed as occurring over two separate stages. In the first stage (cloud formation), those aerosol with radii greater that a certain critical radius grow rapidly by diffusion and condensation to form a spectrum of cloud droplets. Of these newly formed droplets, only those with radii greater than 20 μm will undergo efficient collision-coalescence to produce raindrops (Rogers and Yau, 1989).

In GLOMAP, aerosol with a dry diameter greater than 0.05 μm are assumed able to activate to form cloud drops. During rain formation, the largest of these cloud drops will coalesce most efficiently and will be preferentially lost from the cloud. Following the assumption that the largest aerosol will form the largest cloud droplets (Flossmann, 1991), it can be assumed that in-cloud scavenging will preferentially remove the largest of the activated aerosol. An effective scavenging diameter of 0.206 μm is chosen above which nucleation scavenging may occur in the model, slightly less than the value of 0.250 μm used by Capaldo et al. (1999).

Model sensitivity to the magnitude of the scavenging diameter is investigated by reducing it 0.1 μm. This causes an increase in CN concentrations (between the surface and 20 hPa) of up to 100% and a decrease in CCN concentrations (between the surface and 200 hPa) of up to 50 cm^{-3}. CN concentrations are most affected in the UT whereas CCN concentrations are most affected in the BL. Reducing the scavenging diameter allows more particles to be scavenged, thus more aerosol mass is removed per precipitation event. This reduces aerosol surface area and promotes the nucleation of new

particles. Rates of coagulational scavenging also decrease, allowing more nucleation clusters to survive and grow into CN.

5.4. Sensitivity to particulate sulfate emissions

Here we examine the effect of a small emission of anthropogenic sulfur species in the form of particulates, as has been observed downwind of power plants.

Electricity generation from power plants accounts for a large proportion of anthropogenic emissions of SO_2. In the United States 69% of anthropogenic SO_2 is emitted by coal-fired power plants (EPA, 2000). Emissions of sulfur at the power plant stack are thought to be primarily gaseous SO_2, due to high exhaust temperatures and electrostatic precipitators which remove primary particles (Brock et al., 2002). However, within hours of emission, power plant plumes may experience rapid gas to particle conversion. Brock et al. (2002) measured enhanced particle number concentrations (in the order of 1×10^4 to 1×10^5 cm^{-3}) at distances of 20 to 100 km downwind of coal fired power plants in the eastern United States.

Immediately after emission, high NO concentrations in the plume suppress O_3 and OH concentrations, resulting in a slow rate of oxidation of SO_2 to H_2SO_4 (Brock et al., 2002). As the plume evolves, dilution of NO concentrations and mixing of reactive hydrocarbons from the surrounding air enhances O_3 and OH concentrations particularly at the edges of the plume. This causes the rate of production of H_2SO_4 to increase and if pre-existing particle surface area is low, gas to particle conversion occurs in the plume.

Power plants can therefore cause gas to particle conversion on spatial scales (10 s of km) that are not resolved by global models (with grid squares of 100 km or more). In the model, if SO_2 is simply mixed into a model grid box, the average grid box concentration that is calculated will be an underestimate of the concentrations that are present in the power plant plume before it mixes with the larger scale air masses. If the timescale for oxidation of SO_2 into H_2SO_4 is fast compared to the mixing timescale this may lead to an underprediction of the concentration of gaseous H_2SO_4 in the plume.

ACPD
5, 3437–3489, 2005

In general the average grid box concentrations will not result in any gas to particle conversion. However, the strongly non-linear relationship between H_2SO_4 concentration and nucleation rate may mean that substantial nucleation occurs in the plume. The model which calculates nucleation from average grid point values will underestimate new particle formation that occurs in the power plant plume.

To account for this sub-grid scale particle formation occurring in the plume, a fraction of the total SO_2 emissions into a grid box is assumed to be emitted as particulate sulfate. Estimates of the amount of the emitted SO_2 that forms particulate sulfate in the power plant plume range from less than 1% (Dietz and Wieser, 1983; Eliassen and Saltbones, 1983) to up to 5% (Saeger et al., 1989; EMEP, 1989). Recently, some global aerosol models have attempted to include these direct anthropogenic particulate emissions of sulfate (Gong et al., 2003; Adams and Seinfeld, 2002, 2003). Adams and Seinfeld (2003) reported that neglecting emissions of particulates causes an underprediction of CCN number. Particulate emissions were shown to be more effective at producing CCN than an equivalent amount of gaseous SO_2 emissions.

The effect of including direct particulate emissions in GLOMAP is investigated by comparing model simulations in which all anthropogenic sulfur emissions are assumed to be SO_2 with simulations in which a fraction is assumed to be particulate sulfate. The fraction of SO_2 that is allowed to nucleate in the emission plume is changed from 1 to 5% by mass of total SO_2 emissions. Primary particles are assumed to be formed as two lognormal modes with geometric mean diameters of 10 and 70 nm and standard deviations of 1.6 and 2.0, respectively (Whitby, 1978). Fifteen percent by mass of the primary particles is assumed to be emitted in the small mode and the remainder in the large mode (Binkowski and Shankar, 1995).

Figures 11 and 12 show changes in BL CN and CCN for different fractions of particulate sulfate emission and Fig. 13 shows zonal mean changes. Without direct particulate emissions, surface CN concentrations over polluted regions are typically 1000–2000 cm^{-3}, which is less than typically observed values of 2500–10000 cm^{-3} (Raes et al., 2000). When primary emissions are included, total number concentrations

over polluted areas increase to 2000–10000 cm^{-3}, which is comparable with measurements. Over polluted regions, including particulate emissions increases BL CN concentrations by up to a factor of 10 or more. Surface CN number is increased over a large proportion of the North Atlantic. In comparison, over remote marine and continental regions BL CN concentrations remain relatively unchanged (changing by between 10% and –10%).

CCN concentrations increase from between 500–1000 cm^{-3} to 1000–5000 cm^{-3}. Again there is no simulated effect over remote marine and continental areas. At altitudes above about 400 hPa CCN number is relatively unchanged.

5.5. Sensitivity to sulfur species emission rates

The sensitivity of the simulated aerosol distributions to uncertainty in the emissions database is studied and compared to the sensitivity to uncertainties in the driving microphysical processes.

GLOMAP uses the Global Emissions Inventory Activity (GEIA) for the emissions of anthropogenic SO_2. Benkovitz et al. (1996) attempts to estimate the uncertainty of the GEIA emissions database. Uncertainty is lowest for regions where detailed inventories are available (such as in the US and Europe) and highest where no inventories are available such as over South America and Africa. Uncertainty in regional inventories in Europe (Tuovinen et al., 1994) and the US (Saeger et al., 1989) has been estimated as 25%.

GLOMAP uses the DMS sea-surface concentration database of Kettle et al. (1999) and the sea-air transfer rate from Liss and Merlivat (1986). Uncertainty in the emission rate of DMS is a combination of the uncertainty in DMS sea surface concentrations and the uncertainty in the sea-air transfer rate. The Kettle et al. (1999) database was created using a model that interpolates to a $1^{\circ} \times 1^{\circ}$ grid from more than 15 000 point DMS measurements. The inaccuracy in the database values at any grid point will depend on the sparsity of measurements that are used as input to the mapping algorithm for that

position (Kettle et al., 1999). Uncertainty is generally largest at higher latitudes due to the sparsity of data points and the high spatial and temporal variability in DMS concentrations that occur there. Kettle and Andreae (2000) estimated that overall uncertainty in the sea-air gas flux of DMS is as large as 50%.

To study the effect of these uncertainties in the model, the emission rates for all sulfur-bearing gases were varied by 25% from the baseline emissions. All anthropogenic sulfur was assumed to be gaseous SO_2. This study neglects feedbacks between changes in SO_2 concentrations and gas phase production of H_2O_2.

Figure 14 shows that CN concentrations in the tropical UT between about 200 and 400 hPa and in the NH and SH mid-latitudes are most sensitive to changes in emissions. CCN concentrations are most sensitive to changes in emissions between the surface and about 500 hPa. Changing the emission rate by 25% causes about a 10% change in global mean CN and between 15 and 20% change in global mean CCN concentrations. This change in CCN is larger than the change caused by uncertainties in the nucleation rates (Sect. 5.1), although the changes in CN are less than those due to microphysical processes.

Figure 15 shows the percentage change in global mean CN and CCN concentrations for a 25% and 50% change in global emissions of sulfur gases. Changing the global emission rates has a greater impact on CCN concentrations than CN concentrations. Changing emission rates appears to have an almost linear effect on changes in CCN concentrations. A 50% change in emission rates changes global mean CN concentrations by about 20% and global mean CCN concentrations by about 30–35%, while a 25% change in emission rates changes global mean CN concentrations by about 10% and global mean CCN concentrations by about 15%.

Figure 16 shows number-size distributions and CCN spectra over polluted Northern Europe for different sulfur emission rates and percentage of anthropogenic sulfur emitted as primary particles. In the polluted BL including 1% of sulfur emissions as particulates has a much greater impact on the size distribution than changing emission rates by 25%. When the sulfur flux is changed the general shape of the size distribution

is maintained, but with the distribution shifted up or down in number space. Including a percentage of sulfur emissions as particulates changes both the shape of the distribution and the overall particle concentration below about 1 μm. Over Europe, the number mean diameter shifts from about 50 to 15 nm diameter.

Together, Figs. 13 and 14 help to explain why the size distribution in the polluted BL changes much more in response to primary particles than to greater overall SO_2 emissions. Changing SO_2 leads to small changes in aerosol mass and number right through the troposphere, with peak changes in the UT. In contrast, primary sulfate particles are created immediately in the BL at sizes for which the coagulational scavenging rate is low, so a large fraction of the emitted particles survive.

Over the US both GLOMAP and a limited area model used by von Salzen et al. (2000) show between 30 and 60% decrease in CCN concentrations (depending on the supersaturation) for a 50% decrease in SO_2 emissions.

5.6. Sensitivity to sea spray emission rate

Sea spray particles range in size from 0.02 to 60 μm diameter (Fitzgerald, 1991), but the climatic importance of sea spray through the aerosol indirect effect, depends largely on the number of particles with sizes of 100 to 200 nm diameter (O'Dowd et al., 1999). An accurate description of sea spray flux in this size range is essential to determine the influence of sea spray on the aerosol indirect effect. Under clean marine conditions sea spray particles may dominate the accumulation mode and contribute significantly to the CCN population (O'Dowd and Smith, 1993).

GLOMAP uses the sea spray source function of Gong (2003), which produces realistic fluxes at particle sizes between 0.07 and 20 μm at 80% humidity (corresponding to approximately 0.035 and 10 μm dry diameter). This parameterisation is an extension of the semi-empirical formulation of Monahan et al. (1986) to below 0.2 μm diameter, where the original parametrisation was found to overestimate emissions of sub-micron sea spray particles. The non-dimensional adjustable parameter (Θ) that controls sub-micron emissions is set at 30.

The effect of uncertainty in the sea spray emission flux is investigated by changing the source strength by an order of magnitude. Figure 17 shows that for an order of magnitude increase in sea spray flux, CCN concentrations below about 700 hPa increase by up to 100 cm^{-3}. In remote marine areas this is a larger change in CCN than that caused by changing sulfur gas emission rates by 25%. In the BL, CN concentrations generally increase by less than 5% for an order of magnitude increase in sea spray emissions, although changes of up to 10% between 40 and 60° S are predicted. Changes in CN are negligible above the BL.

Figure 18 compares the effect on North Atlantic and Southern Ocean MBL number-size distributions of changing sulfur and sea spray emissions. There is an obvious difference between the two oceans in the number of particles in the accumulation mode (~100–200 nm). In the North Atlantic, the accumulation mode is dominated by sulfate aerosol, and even large increases in sea spray flux have little impact. In contrast, the Southern Ocean accumulation mode number increases from ~10–50 cm^{-3} to ~100–250 cm^{-3} for an order of magnitude increase in sea spray emissions. Accumulation mode number in the Southern Ocean is also sensitive to the value of Θ (non-dimensional) in the paramateristaion of Gong et al. (2003). Changing Θ from 40 to 15 causes an order of magnitude increase in sub-micron sea spray emissions and an increase in accumulation mode number to about 50–100 cm^{-3}. In both oceans the increase in accumulation mode number is largely offset by decreases in Aitken number, and so total number remains relatively unchanged. Reductions in Aitken mode particle concentrations are caused by the increase in the BL coagulation sink causing faster scavenging of smaller particles.

Our simulations show that switching off sea spray flux changes global mean CN number by less than 1% (not shown). This result is different to that obtained by Gong and Barrie (2003), who saw BL number increase between 30 and 50% in the North Atlantic and Southern Oceans when no sea spray emissions were included. When the sea spray emission flux is turned off in GLOMAP there is still sufficient nss-sulfate aerosol in the BL to provide the necessary condensation sink to keep gas-phase H_2SO_4

concentrations below the binary H_2SO_4–H_2O nucleation threshold. Aerosol nucleation occurs predominantly in the cold FT and UT in GLOMAP, but the short lifetime of sea spray is such that only a very small fraction is transported into these cold regions. CN concentrations in the UT, and hence the rate of entrainment of aerosol from the FT to the BL, is therefore not changed when the sea spray emission flux is reduced.

The different response of CN to changes in sea spray in our simulations and those of Gong and Barrie (2003) is due to the different H_2SO_4 accommodation coefficients used. Figure 19 shows the effect of changes in sea spray emissions on vertical profiles of CN number over the Southern Ocean for different accommodation coefficients. When a_e is reduced to 0.02 (as used by Gong and Barrie (2003)), removing sea spray emissions causes an increase in BL CN number of about 50%. Such a low value of a_e in GLOMAP allows nucleation to occur much closer to the surface (see Sect. 5.1.1) so when sea salt emissions are reduced the reduction in the coagulation sink allows more of these particles to survive to CN sizes.

6. Summary

The sensitivity of the sulfate and sea salt aerosol size distribution and the spatial distributions of CN and CCN abundances to changes in the rates of microphysical processes and emission strengths has been investigated using a global model with a sectional aerosol scheme.

The sensitivity of sulfate and sea salt CN and CCN concentrations is summarised in Fig. 20. In general, model predictions of CN and CCN concentrations are sensitive to realistic uncertainties in both emissions and microphysical processes. Global mean CN concentrations are dominated in these simulations by the very high concentrations of sulfuric acid aerosol in the free and upper troposphere where nucleation rates are highest. Global mean CN is therefore sensitive to the rate of nucleation, the critical cluster size and the accommodation coefficient of sulfuric acid but relatively insensitive to the activation process in clouds or the emission of primary sulfate particle from sur-

face sources. Global CN is also sensitive to the process of wet scavenging of aerosol, which controls the particle surface area in the FT and UT, and hence the competition for available sulfuric acid vapor between particle formation and condensation to existing particles.

Global mean surface CN concentrations in these simulations are dominated by sulfuric acid aerosol and are most sensitive to uncertainties in primary sulfate emissions and the accommodation coefficient. The lowest value of the sulfuric acid accommodation coefficient used here (a_e=0.02) is probably an extreme choice, although even a modest value of 0.3 (decreased from 1.0) increases surface mean CN concentrations by 69%. Primary sulfate emissions have the potential to change the global mean surface sulfate CN concentration by a factor 2 or more, and changes of up to a factor 20 can occur in polluted regions. CN are also produced from non-sulfate sources. Further studies involving more aerosol types and sources are needed to put these sensitivities in context.

Predicted global mean sulfate and sea salt CCN concentrations at the surface change by 10 to 40% when several microphysical processes are changed within reasonable uncertainty ranges, and these microphysical uncertainties have a similar effect on CCN to uncertainties in emissions of sulfur species. Cloud processes are very important in controlling CCN concentrations. Aerosol processing through clouds (causing mass addition to aerosols by SO_2 oxidation in droplets) moves aerosols from Aitken mode sizes to the accumulation mode more rapidly than is achieved through condensation of sulfuric acid and coagulation. We have investigated how uncertainties in the activation diameter of aerosols in clouds affects CCN at a particular supersaturation. The activation diameter is in reality controlled by cloud-scale updraught velocities, which are difficult to predict in global models. Reasonable uncertainties in the activation diameter in our model lead to changes in global mean surface level CCN concentrations of as much as 35% at a given supersaturation. Scavenging of aerosol by precipitating clouds also exerts a strong control on CCN abundances.

CCN concentrations are particularly sensitive to assumptions made about the pro-

duction of primary sulfate particles in pollution plumes below the scale of the model grid. Reasonable assumptions about the grid-mean concentration of such particles leads to uncertainties in global mean CCN of as much as 40%, with local changes of more than 100% in polluted regions. This uncertainty is larger than the change in CCN (about ±15% global mean) caused by a ±25% change in total sulfur emissions. Our model therefore suggests that the mode of sulfate emission is as important for CCN abundance as the magnitude. A large fraction of CCN-sized particles are likely to be composed of material other than sulfate and sea salt over continental regions. These estimates of CCN sensitivity therefore need to be repeated in a model with a more complete range of aerosol types.

We have also shown that the altitude of the upper tropospheric CN layer is sensitive to a number of microphysical processes. Changes in the nucleation rate, the condensation rate and the size of freshly nucleated clusters within realistic ranges leads to changes in the altitude of peak CN concentrations by up to 3 km. Variations in the nucleation and condensation rate change the CN altitude without changing CN concentrations, while changes in the cluster size change both the altitude and the peak concentration. The simulated altitude of the CN layer may be a better measure of model quality than absolute concentrations.

7. Implications and outlook

This study has focussed on the uncertainty in CN and CCN concentrations due to realistic uncertainties in the microphysical processes that control the size distribution of sulfate and sea salt aerosol. One might argue that the use of a global aerosol microphysics model (as opposed to a simpler aerosol parameterisation in a climate model) has simply extended the list of uncertain parameters without actually reducing the overall uncertainty. At this stage in the development and evaluation of aerosol microphysics models, this is true. However, it needs to be remembered that, ultimately, it is changes in the particle size distribution that determine the magnitude of the direct and indirect

aerosol forcing. Our understanding of what controls changes in the aerosol size distribution is far from complete. Without such understanding we are not in a position to say that changes in forcing in the industrial period can be accurately predicted using models that simulate only aerosol mass, which has been assumed in climate change attribution studies to date (IPCC, 2002). The temporal pattern of radiative forcing over the last 100 years is critical for the attribution of climate change. Further development of such microphysical models, the addition of more aerosol components, and the improvement of schemes to treat the most uncertain processes is therefore essential.

The uncertainties in predicted CCN are large compared with changes that are likely to be important for the aerosol direct and indirect radiative forcing (Pan et al., 1997, 1998). For example, changes in lower atmospheric global mean cloud drop number in response to changing aerosol emissions since 1860 are predicted by general circulation models to be of the order 70% (A. Jones, pers. comm.). We estimate the uncertainty in global mean sulfate and sea salt CCN concentrations to be as much as 40%, although the uncertainty in total CCN may be lower in a model that considers the complete range of primary aerosol emissions.

A useful extension to this work in the context of climate change would be to quantify the extent to which these uncertainties restrict our ability to quantify *changes* in radiative forcing and cloud properties in response to changes in emissions. For example, whether the response of CCN to changes in sulfur emissions is different when high or low nucleation rates are used or if high or low primary sulfate emissions are assumed. We also need to determine whether any of these microphysical processes or the nature of emissions has changed over the last 100 years. For example, the contribution of primary sulfate aerosol to boundary layer CCN is likely to have changed as emissions have shifted from domestic sources to power plants. Such changes may have as important an effect on radiative forcing as gross changes in emissions themselves. Neither of these processes affecting particle number can be studied with a mass-only aerosol scheme.

Our work points towards a number of processes that require better representation in

global model. The bulk of the uncertainty in predicted sulfate and sea salt CCN concentrations arises from the contribution of primary sulfate particles to the grid mean in the model and from the uncertainty in the effect of clouds on the aerosol size distribution. Both of these processes present a particularly challenging problem for global models. Accurate descriptions of cloud processes will be essential for quantitative estimates of global CCN number.

Conclusions regarding the most important uncertainties are valid only in so far as the mechanisms used in the model are realistic. In particular, our model assumes that binary homogeneous nucleation of sulfuric acid-water aerosol is the only particle formation mechanism. Because the nucleation rate according to this mechanism peaks at the low temperatures in the upper troposphere, our simulations suggest that boundary layer aerosol is relatively insensitive to the nucleation rates. However, observations and model studies suggest that particle formation can occur in the continental boundary layer, perhaps accelerated by the presence of gaseous organic compounds (Antilla et al., 2004). In Sect. 5.4 we stated that our model tends to under-predict continental boundary layer CN concentrations and that this discrepancy may be accounted for by primary sulfate particles. However, alternative aerosol nucleation mechanisms may also help to explain such discrepancies. Much work is needed to identify the mechanism of particle formation throughout the atmosphere so that we can understand observed aerosol abundances and predict changes.

References

Adams, P. and Seinfeld, J.: Predicting global aerosol size distributions in general circulation models, J. Geophys. Res.-Atmos., 107, 4370–4393, 2002. 3439, 3440, 3446, 3454

Adams, P. and Seinfeld, J.: Disproportionate impact of particulate emissions on global cloud condensation nuclei concentrations, Geophys. Res. Lett., 30, 43–46, 2003. 3439, 3454

Antilla, T., Kerminen, V.-M., Kulmala, M., Laaksonen, A., and O'Dowd, C.: Modelling the formation of organic particles in the atmosphere, Atmos. Chem. Phys., 4, 1071–1083, 2004, SRef-ID: 1680-7324/acp/2004-4-1071. 3463

Ayers, G. and Gillett, R.: DMS and its oxidation products in the remote marine atmosphere: implications for climate and atmospheric chemistry, Jornal of Sea Research, 43, 275–286, 2000. 3451

Benkovitz, C., Scholtz, M., Pacyna, J., Tarrasón, L., Dignon, J., Voldner, E., Spiro, P., Logan, J., and Graedel, T.: Global gridded inventories of anthropogenic emissions of sulfur and nitrogen, J. Geophys. Res.-Atmos., 101, 29 239–29 253, 1996. 3455

Binkowski, F. and Shankar, U.: The regional particulate matter model, 1, Model description and preliminary results, 100, J. Geophys. Res.-Atmos., 26 191–26 209, 1995. 3454

Boucher, O. and Anderson, T.: General circulation model assessment to the sensitivity of direct climate forcing by anthropogenic sulfate aerosols to aerosol size and chemistry, J. Geophys. Res.-Atmos., 100, 26 117–26 134, 1995. 3440

Brock, C., Washenfelder, R., Trainer, M., Ryerson, T., Wilson, J., Reeves, J., Huey, L., Holloway, J., Parrish, D., Hübler, G., and Fehsenfeld, F.: Particle growth in the plumes of coal-fired power plants, J. Geophys. Res.-Atmos., 107, 4155–4169, 2002. 3453

Capaldo, K., Kasibhatla, P., and Pandis, S.: Is aerosol production within the marine boundary layer sufficient to maintain observed concentrations?, J. Geophys. Res.-Atmos., 104, 3483–3500, 1999. 3440, 3452

Clarke, A., Varner, J., Eisele, F., Mauldin, R., Tanner, D., and Litchy, M.: Particle production in the remote marine atmosphere: Cloud outflow and subsidence during ACE 1, J. Geophys. Res.-Atmos., 103, 16 397–16 409, 1998. 3445

Clement, C., Kulmala, M., and Vesala, T.: Theoretical considerations on sticking probabilities, J. Aerosol Sci., 27, 869–882, 1996. 3446

Coffman, D. and Hegg, D.: A preliminary study of the effect of ammonia on particle nucleation in the marine boundary layer, J. Geophys. Res.-Atmos., 100, 7147–7160, 1995. 3445

Däumer, B., Niessner, R., and Klockow, C.: Laboratory studies of the influence of thin organic films on the neutralization reaction of H_2SO_4 aerosol with ammonia, Journal of Aerosol Science, 23, 315–325, 1992. 3447

Dietz, R. and Wieser, R.: Sulfate formation in oil fired power plant plumes, Volume 1: Parameters affecting primary sulfate emissions and a model for predicting emissions and plume opacity, Tech. rep., Electric Power Research Institute, 1983. 3454

Easter, R. and Peters, L.: Binary homogeneous nucleation: Temperature and relative humidity fluctuations, non-linearity and aspects of new particle production in the atmosphere, J. Appl. Meteorol., 33, 775–784, 1994. 3445

Easter, R., Ghan, S., Zhang, Y., Saylor, R., Chapman, E., Laulainen, N., Abdul-Razzak, H., Leung, L., Bian, X., and Zaveri, R.: MIRAGE: Model description and evaluation of aerosols and trace gases, J. Geophys. Res.-Atmos., 109, doi:10.1029/2004JD004 571, 2004. 3446

Eliassen, A. and Saltbones, J.: Modelling of long range transport of sulfur over Europe: A two year model run and some model experiments, Atmos. Environ., 17, 1457–1473, 1983. 3454

EMEP: Airborne transboundary transport of sulfur and nitrogen species over Europe – model descriptions and calculations, Tech. Rep. 80, EMEP, 1989. 3454

EPA: National air quality and emissions trends report, Tech. Rep. Rep. EPA 454/R-00-0003, Environmental Protection Agency, 2000. 3453

Fitzgerald, J.: Marine aerosols: A review, Atmos. Environ., 25, 533–545, 1991. 3457

Flossmann, A.: The scavenging of 2 different types of marine aerosol-particles calculated using a 2-dimensional detailed cloud model, Tellus, 43, 301–321, 1991. 3452

Gong, S.: A parameterization of sea-salt aerosol source function for sub- and super-micron particles, Global Biogeochemical Cycles, 17, 1097–1103, 2003. 3457

Gong, S. and Barrie, L.: Simulating the impact of sea salt on global nss sulphate aerosols, J. Geophys. Res.-Atmos., 108, 4516–4533, 2003. 3458, 3459

Gong, S., Barrie, L., and Blanchet, J.-P.: Modeling sea-salt aerosols in the atmosphere. 1. Model Development, J. Geophys. Res.-Atmos., 102, 3805–3818, 1997. 3439

Gong, S., Barrie, L., Blanchet, J.-P., von Salzen, K., Lohmann, U., Lesins, G., Spacek, L., Zhang, L., Girard, E., Lin, H., Leaitch, R., Leighton, H., Chylek, P., and Huang, P.: Canadian Aerosol Module: A size-segregated simulation of atmospheric aerosol processes for climate and air quality models, 1. Module development, J. Geophys. Res.-Atmos., 108, 4007–4023, 2003. 3439, 3454, 3458

Gras, J.: CN, CCN and particle size in Southern Ocean air at Cape Grim, Atmospheric Research, 35, 233–251, 1995. 3451

Hoppel, W., Frick, G., and Larson, R.: Effect of nonprecipitating clouds on the aerosol size distribution, Geophys. Res. Lett., 13, 125–128, 1986. 3442

Jacobson, M. Z.: GATOR-GCMM: A global- through urban -scale air pollution and weather forecast model, 1. Model design and treatment of subgrid soil, vegetation, roads, rooftops, water, sea ice, and snow, J. Geophys. Res.-Atmos., 106, 5385–5401, 2001. 3439

Jefferson, A., Eisele, F., Ziemann, P., Weber, R., Marti, J., and McMurry, P.: Measurements of the H_2SO_4 mass accommodation coefficient onto polydisperse aerosol, J. Geophys. Res.-Atmos., 102, 19 021–19 028, 1997. 3446

Katoshevski, D., Nenes, A., and Seinfeld, J.: A study of processes that govern the maintenance of aerosols in the marine boundary layer, J. Aerosol Sci., 30, 503–532, 1999. 3446
Kerminen, V.-M. and Wexler, A.: Growth behavior of the marine submicron boundary layer aerosol, J. Geophys. Res.-Atmos., 102, 18 813–18 825, 1997. 3440
Kettle, A. and Andreae, M.: Flux of dimethylsulfide from the oceans: A comparison of updated data sets and flux models, J. Geophys. Res.-Atmos., 105, 26 793–26 808, 2000. 3456
Kettle, A., Andreae, M., Armouroux, D., Andreae, T., Bates, T., Berresheim, H., Bingemer, H., Boniforti, R., Curran, M., DiTullio, G., Helas, G., Jones, G., Keller, M., Kiene, R., Leck, C., Levasseur, M., Malin, G., Maspero, M., Matrai, P., McTaggart, A., Mihalopoulos, N., Nguyen, B., Novo, A., Putaud, J., Rapsomanikis, S., Roberts, G., Schebeske, G., Sharma, S., Simö, R., Staubes, R., Turner, S., and Uher, G.: A global database of sea surface dimethylsulfide (DMS) measurements and a procedure to predict sea surface DMS as a function of latitude, longitude and month, Global Biogeochemical Cycles, 13, 399–444, 1999. 3455, 3456
Kiehl, J. and Briegleb, B.: The relative roles of sulfate aerosols and greenhouse gases in climate forcing, Science, 260, 311–314, 1993. 3440
Kulmala, M., Laaksonen, A., and Pirjola, L.: Parameterizations for sulfuric acid/water nucleation rates, J. Geophys. Res.-Atmos., 103, 8301–8307, 1998. 3445, 3446, 3449, 3471, 3472
Kulmala, M., Vehkamäki, H., Petajda, T., Dal Maso, M., Lauri, A., Kerminen, V., Birmili, W., and McMurry, P.: Formation and growth rates of ultrafine atmospheric particles: a review of observations, Journal of Aerosol Science, 35, 143–176, 2004. 3445, 3449
Liss, P. and Merlivat, L.: The Role of Air-Sea Exchange in Geochemical Cycling, chap. Air-sea gas exchange rates: Introduction and synthesis, D. Reidel, Norwell, Mass., 113–127, 1986. 3455
Marti, J., Jefferson, A., Cai, X., Richert, C., McMurry, P., and Eisele, F.: H_2SO_4 vapour pressure of sulfuric acid and ammonium sulfate solutions, J. Geophys. Res.-Atmos., 1997. 3445
McMurry, P.: A review of atmospheric aerosol measurements, Atmospheric Environment, 2000. 3441
Monahan, E., Spiel, D., and Davidson, K.: Oceanic Whitecaps, chap. A model of marine aerosol generation via whitecaps and wave disruption, D. Reidel, Norwell, Mass., 167–174, 1986. 3457
Myhre, G., Stordal, F., Berglen, T., Sundet, J., and Isaksen, I.: Uncertainties in the Radiative Forcing Due to Sulfate Aerosols, Journal of the Atmospheric Sciences, 61, 485–498, 2004. 3440

Napari, I., Noppel, M., Vehkamäki, H., and Kulmala, M.: An improved model for ternary nucleation of sulfuric acid-ammonia-water, J. Chem. Phys., 2002. 3445

Nemesure, S., Wagener, R., and Schwartz, S.: Direct radiative forcing of climate by the anthropogenic sulfate aerosol: Sensitivity to particle size, composition and relative humidity, J. Geophys. Res.-Atmos., 100, 26 105–26 116, 1995. 3440

Nilsson, E., Pirjola, L., and Kulmala, M.: The effect of atmospheric waves on aerosol nucleation and size distribution, J. Geophys. Res.-Atmos., 105, 19 917–19 926, 2000. 3445

O'Dowd, C. and Smith, M.: Pysio-chemical properties of aerosols over the North Atlantic: Evidence for wind-speed related submicron sea-salt aerosol production, J. Geophys. Res.-Atmos., 98, 1137–1149, 1993. 3457

O'Dowd, C., Lowe, J., Smith, M., and Kaye, A.: The relative importance of non-sea-salt sulphate and sea-salt aerosol to the marine cloud condensation nuclei population: An improved multi-component aerosol-cloud droplet parametrization, Q. J. R. Meteorol. Soc., 125, 1295–1313, 1999. 3457

Pan, W., Tatang, M., McRae, G., and Prinn, R.: Uncertainty analysis of direct radiative forcing by anthropogenic sulfate aerosols, J. Geophys. Res.-Atmos., 102, 21 915–21 924, 1997. 3440, 3462

Pan, W., Tatang, M., McRae, G., and Prinn, R.: Uncertainty analysis of indirect radiative forcing by anthropogenic sulfate aerosols, J. Geophys. Res.-Atmos., 103, 3815–3823, 1998. 3440, 3462

Pandis, S., Russell, L., and Seinfeld, J.: The relationship between DMS flux and CCN concentration in remote marine regions, J. Geophys. Res.-Atmos., 99, 16 945–19 957, 1994. 3440, 3446

Pilinis, C., Pandis, S., and Seinfeld, J.: Sensitivity of direct climate forcing by atmospheric aerosols to aerosol size and composition, J. Geophys. Res.-Atmos., 100, 18 739–18 754, 1995. 3440

Poschl, U., Canagaratna, M., Jayne, J., Molina, L., Worsnop, D., Kolb, C., and Molina, M.: Mass accommodation coefficient of H_2SO_4 vapour on aqueous sulfuric acid surfaces and gaseous difussion coefficient of H_2SO_4 in N_2/H_2O, J. Phys. Chem. A, 102, 10 082–10 089, 1998. 3446

Raes, F.: Entrainment of free tropsospheric aerosols as a regulating mechanism for cloud condensation nuclei in the remote marine boundary layer, J. Geophys. Res.-Atmos., 100, 2893–2903, 1995. 3440, 3446

Raes, F., Van Dingenen, R., Vignati, E., Wilson, J., Putaud, J.-P., Seinfeld, J., and Adams,

P.: Formation and cycling of aerosols in the global troposphere, Atmos. Environ., 34, 4215–4240, 2000. 3454
Rogers, R. and Yau, M.: Short course in cloud physics, chap. Formation of cloud drops, Elsevier Science Ltd., 1989. 3452
Russell, L., Pandis, S., and Seinfeld, J.: Aerosol production and growth in the marine boundary layer, J. Geophys. Res.-Atmos., 99, 20 989–21 003, 1994. 3446
Saeger, M., Langstaff, J., Walters, R., Modica, L., Zimmerman, D., Fratt, D., Dulleba, D., Ryan, R., Demmy, J., Tax, W., Sprague, D., Mudgett, D., and Werner, A.: Development of the annual data and modelers' tape, Tech. rep., US Environmental Protection Agency, 1989. 3454, 3455
Spracklen, D., Pringle, K., Carslaw, K., Chipperfield, M., and Mann, G.: A global off-line model of size resolved aerosol processes; I. Model development and prediction of aerosol properties, Atmos. Chem. Phys. Discuss., 5, 179–215, 2005, SRef-ID: 1680-7375/acpd/2005-5-179. 3439, 3441, 3445, 3446
Stockwell, D. and Chipperfield, M.: A tropospheric chemical-transport model: Development and validation of the model transport schemes, Q. J. R. Meteorol. Soc., 125, 1747–1783, 1999. 3441
Stolzenburg, M. and McMurry, P.: An ultrafine aerosol condensation nucleus counter, Aerosol Sci. Tech., 14, 48–65, 1991. 3441
Tuovinen, J.-P., Banett, K., and Styve, H.: Transboundary Acidifying Pollution in Europe: Calculated Fields and Budgets 1985-93, Tech. rep., The UN Economic Commission for Europe (ECE) Cooperative Programme for Monitoring and Evaluation of the Long Range Transmission of Air Pollutants in Europe. Oslo, 1994. 3455
Van Dingenen, R. and Raes, F.: Determination of the condensation accommodation coefficient of sulfuric acid on water-sulfuric acid aerosol, Aerosol Sci. Technol., 15, 93–106, 1991. 3446
Vehkamäki, H., Kulmala, M., Napari, I., Lehtinen, K., Timmreck, C., Noppel, M., and Laaksonen, A.: An improved parametrization for sulfuric acid-water nucleation rates for tropospheric and stratospheric conditions, J. Geophys. Res.-Atmos., 107, 4622–4631, 2002. 3445, 3449
von Salzen, K., Leighton, H., Ariya, P., Barrie, L., Gong, S., Blanchet, J.-P., Spacek, L., Lohmann, U., and Kleinman, L.: Sensitivity of sulphate aerosol size distributions and CCN concentrations over North America to SO_x emissions and H_2O_2 concentrations, J. Geophys. Res.-Atmos., 105, 9741–9765, 2000. 3457
Weber, R., McMurry, P., Eisele, F., and Tanner, D.: Measurement of expected nucleation precur-

sor species and 3–500 nm diameter particles at Mauna Loa Observatory, Hawaii, J. Atmos. Sci., 52, 2242–2256, 1995. 3445, 3446

Whitby, K.: The physical characteristics of sulfur aerosols, Atmos. Environ., 12, 135–159, 1978. 3454

Yoon, Y. and Brimblecombe, P.: Modelling the contribution of sea salt and dimethyl sulfide derived aerosol to marine CCN, Atmos. Chem. Phys., 2, 17–30, 2002, SRef-ID: 1680-7324/acp/2002-2-17. 3440

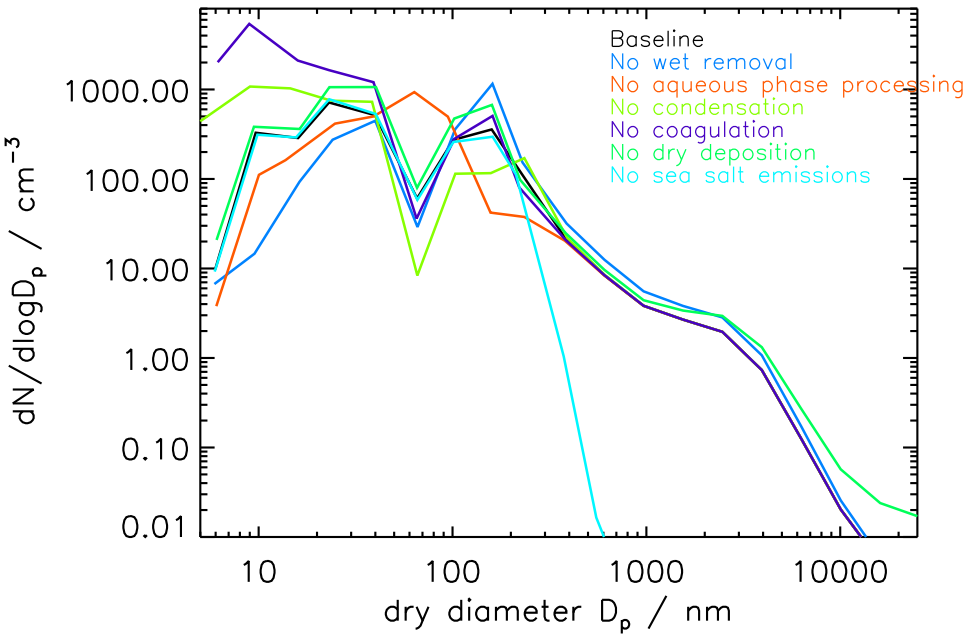

Fig. 1. Comparison of twenty four hour average number-size distributions for the North Atlantic MBL during December 1995 with all microphysical processes included and when one microphysical process at a time has been switched off for the last eight days of the model run.

ACPD
5, 3437–3489, 2005

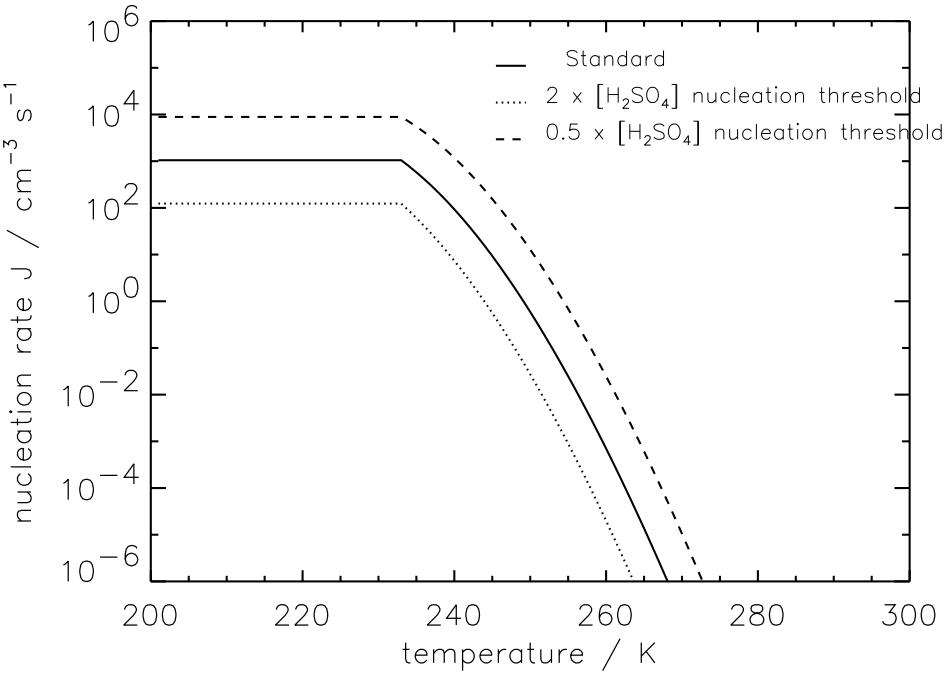

Fig. 2. Calculated nucleation rates using the Kulmala et al. (1998) paramaterisation for a fixed gas phase H_2SO_4 concentration of 3×10^7 cm^{-3} and relative humidity of 55%. Below 233 K the nucleation rate is held constant.

ACPD
5, 3437–3489, 2005

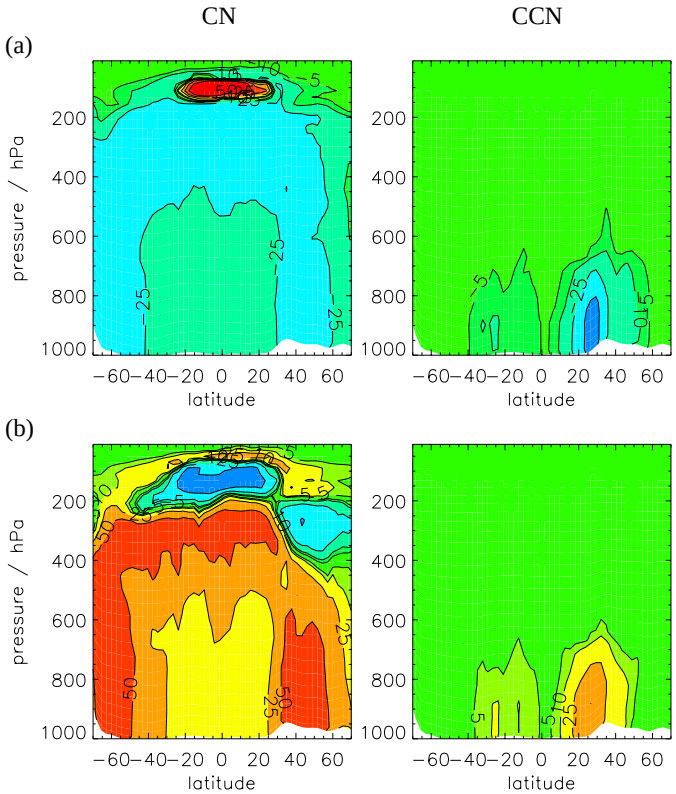

Fig. 3. Monthly mean change in zonal mean CN (% change) and CCN (absolute change (cm^{-3}) at 0.2% supersaturation) at STP for December 1995 for **(a)** H_2SO_4 threshold twice that of baseline case; **(b)** H_2SO_4 threshold half that of baseline case. A doubling/halving of the threshold H_2SO_4 concentration for nucleation in the Kulmala et al. (1998) parameterisation causes approximately a factor 10 decrease/increase in the nucleation rate under most conditions (see Sect. 5.1.1).

ACPD
5, 3437–3489, 2005

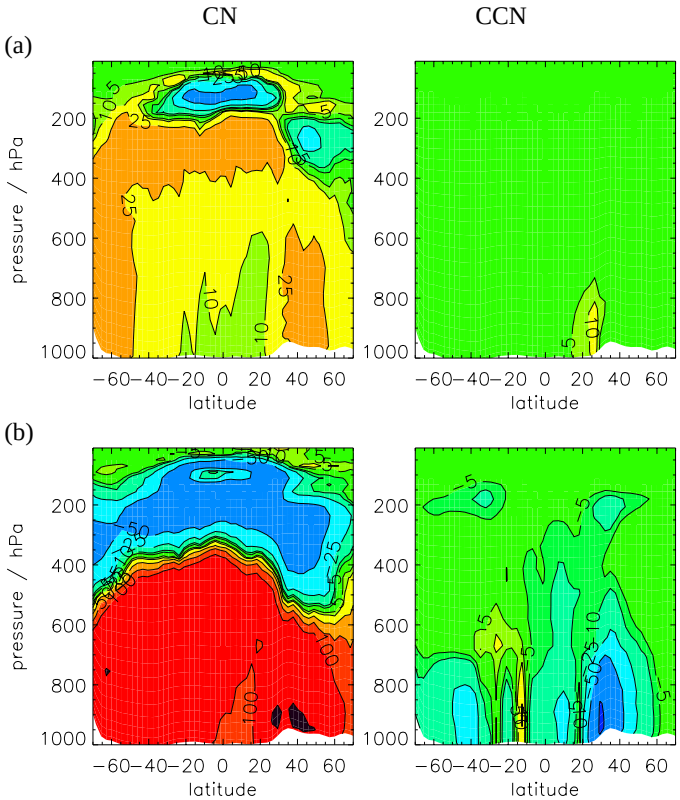

Fig. 4. Monthly mean change in zonal mean CN (percentage change) and CCN (absolute change (cm^{-3}) at 0.2% supersaturation) at STP for December 1995 for accommodation coefficients of **(a)** a_e=0.65; **(b)** a_e=0.02. Baseline model runs use a_e=1.0

ACPD
5, 3437–3489, 2005

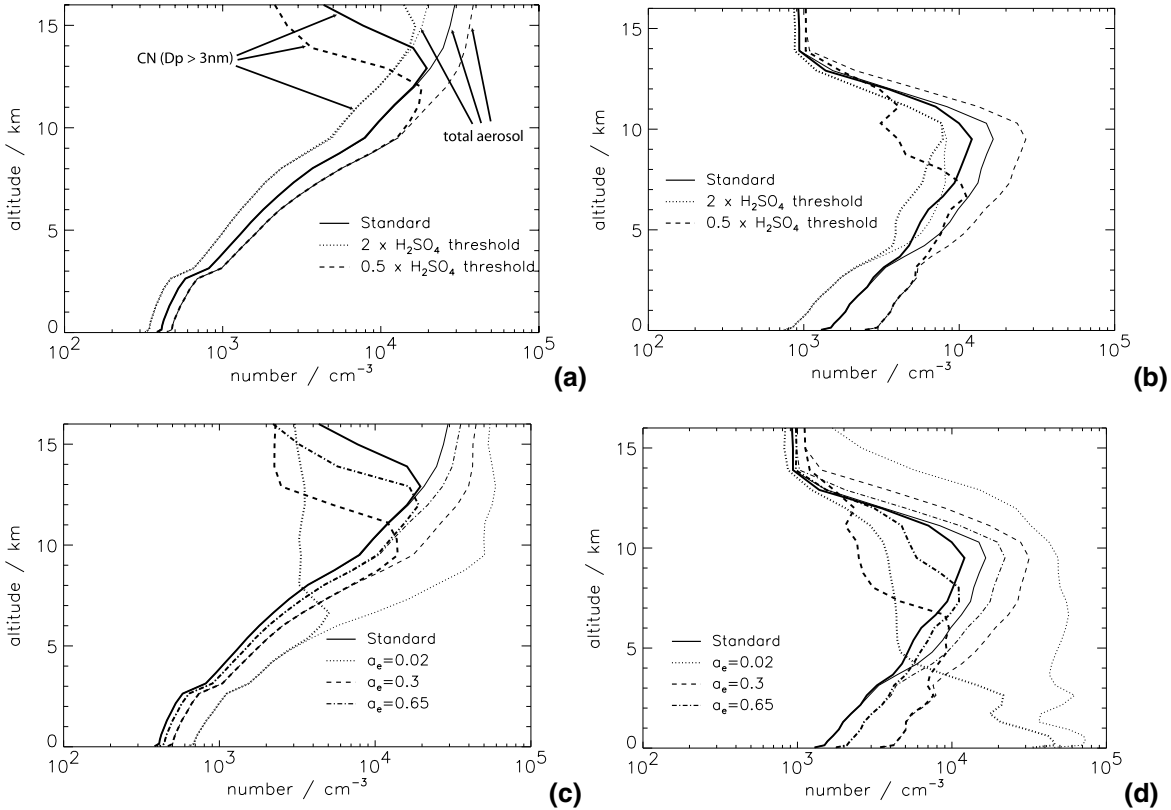

Fig. 5. Monthly mean vertical profiles for December 1995 for changes in nucleation and condensation rate. Number concentration (at STP) are shown for particles with dry diameter greater than 3 nm (thick lines) and all particles including nucleation clusters less than 3 nm diameter (thin lines).

ACPD
5, 3437–3489, 2005

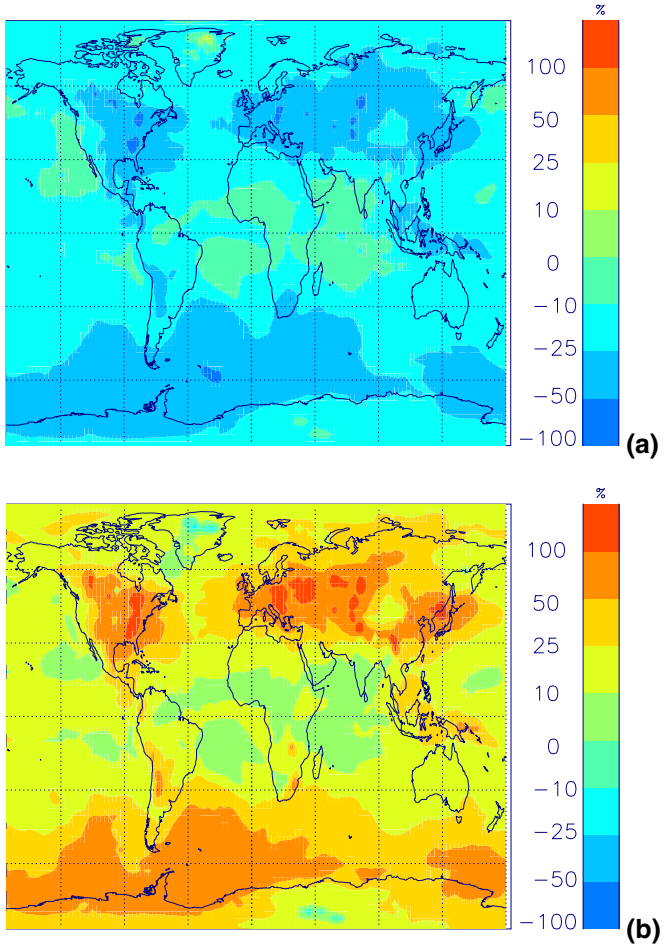

Fig. 6. Monthly mean percentage change in surface mean CN concentrations for December 1995. **(a)** H_2SO_4 threshold twice that of baseline case; **(b)** H_2SO_4 threshold half that of baseline case.

ACPD
5, 3437–3489, 2005

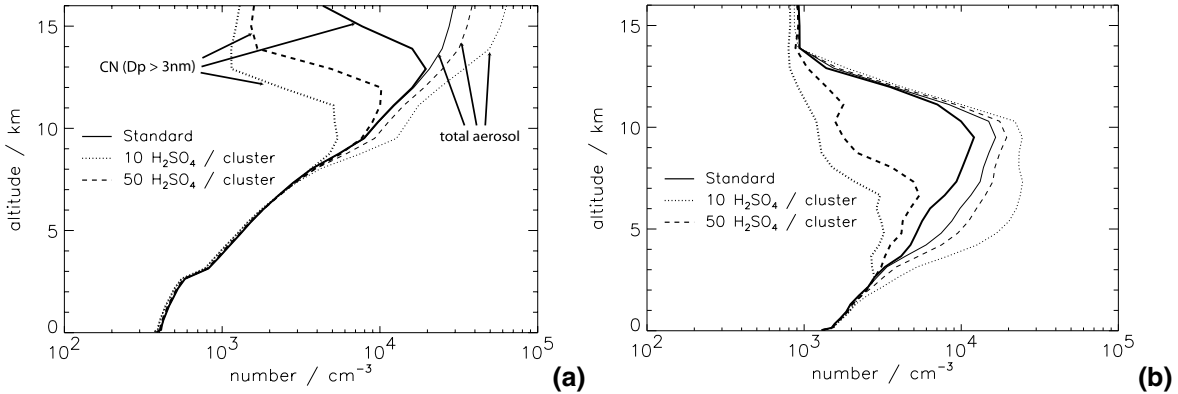

Fig. 7. Monthly mean vertical profiles during December 1995 for different H_2SO_4 nucleation cluster sizes. Number concentration (at STP) are shown for particles with dry diameter greater than 3 nm (thick lines) and all particles including nucleation clusters less than 3 nm diameter (thin lines).

ACPD
5, 3437–3489, 2005

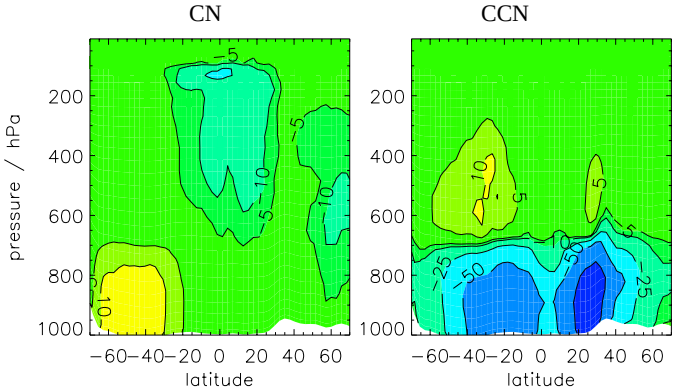

Fig. 8. Monthly mean change in zonal mean CN (% change) and CCN (absolute change (cm^{-3}) at 0.2% supersaturation) concentrations at STP for December 1995 for an aerosol activation diameter into cloud droplets of 0.08 μm. Baseline activation diameter is 0.05 μm.

ACPD
5, 3437–3489, 2005

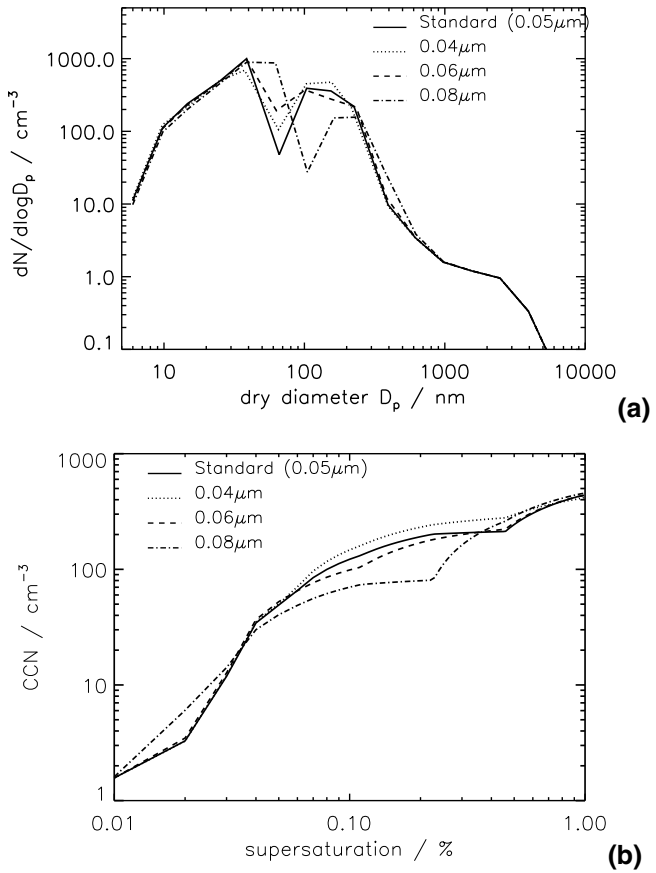

Fig. 9. Monthly mean simulated aerosol distributions in the tropical Pacific MBL (10° N–10° S, 210–270° E) for December 1995 with different activation diameters for aqueous phase oxidation. **(a)** number-size distribution; **(b)** CCN spectrum.

ACPD
5, 3437–3489, 2005

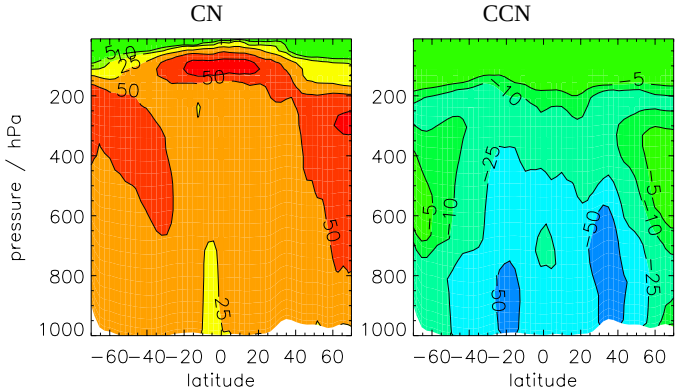

Fig. 10. Monthly mean change in zonal mean CN (% change) and CCN (absolute change (cm^{-3}) at 0.2% supersaturation) concentrations at STP for activation diameters into cloud droplets for nucleation scavenging of 0.1 μm. Baseline activation diameter is 0.206 μm.

ACPD
5, 3437–3489, 2005

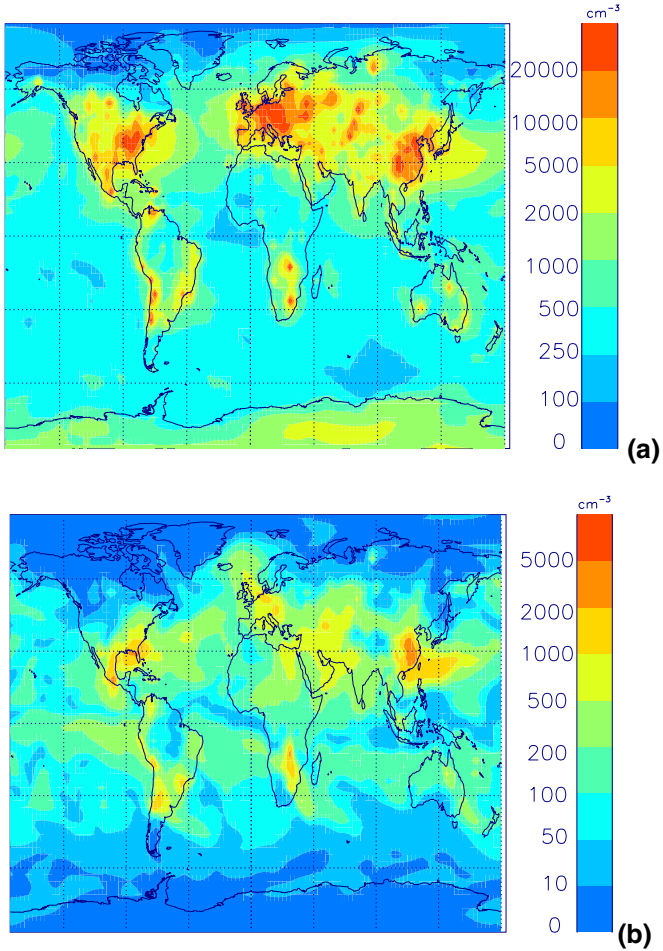

Fig. 11. Monthly mean surface **(a)** CN and **(b)** CCN (0.2% supersaturation) concentrations for December 1995 with 3% of SO_2 as particulate emissions.

ACPD
5, 3437–3489, 2005

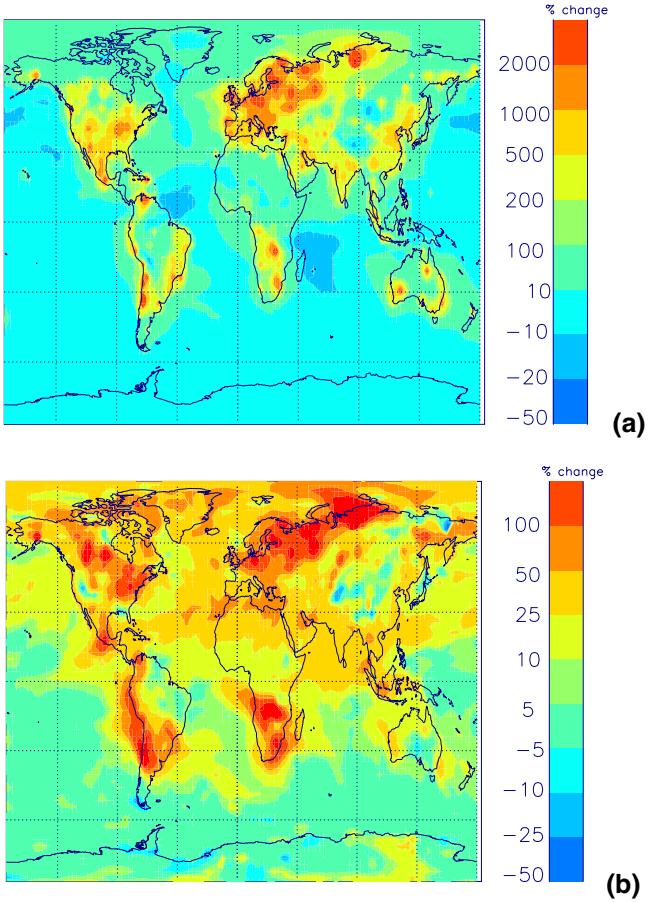

Fig. 12. Monthly mean percentage change in surface (a) CN and (b) CCN (0.2% supersaturation) concentrations for 3% SO_2 emitted as particulate sulfate compared to model run with 100% of emissions as SO_2.

ACPD
5, 3437–3489, 2005

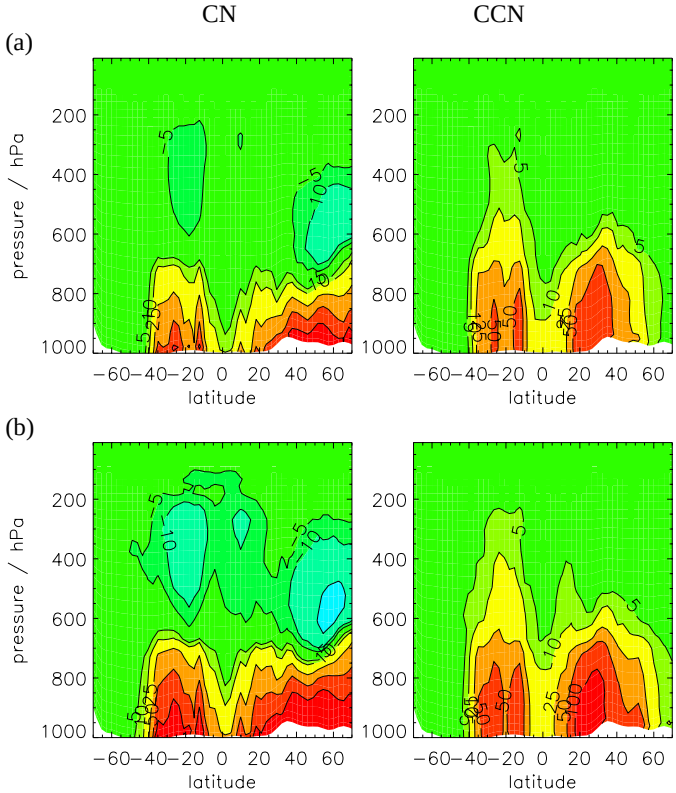

Fig. 13. Monthly mean change in zonal mean CN (% change) and CCN (absolute change cm^{-3} at 0.2% supersaturation) concentrations at STP for December 1995. **(a)** 1% direct particulate emissions; **(b)** 3% direct particulate emission.

ACPD
5, 3437–3489, 2005

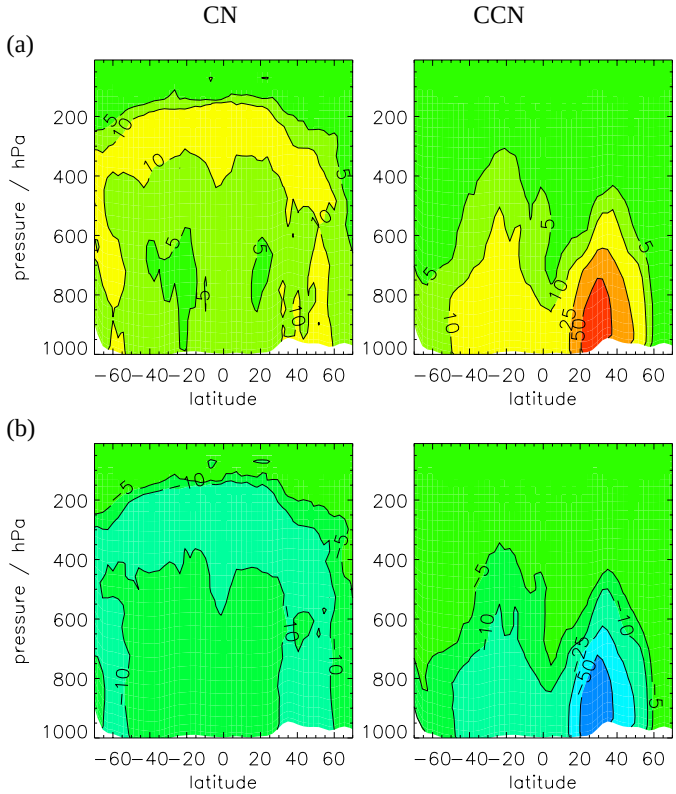

Fig. 14. Monthly mean change in zonal mean CN (% change) and CCN (absolute change (cm^{-3}) at 0.2% supersaturation) concentrations for December 1995. **(a)** all sulfur emissions 125% of the baseline emissions; **(b)** all sulfur emissions 75% of the baseline emissions.

ACPD
5, 3437–3489, 2005

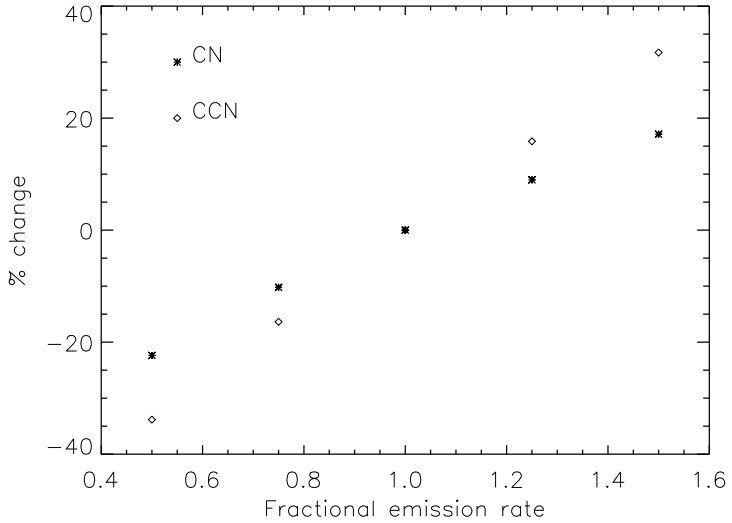

Fig. 15. Percentage change in global average monthly mean CN and CCN (0.2% supersaturation) concentrations for December 1995 for sulfur emission rates of between 50% and 150% of baseline emissions.

ACPD
5, 3437–3489, 2005

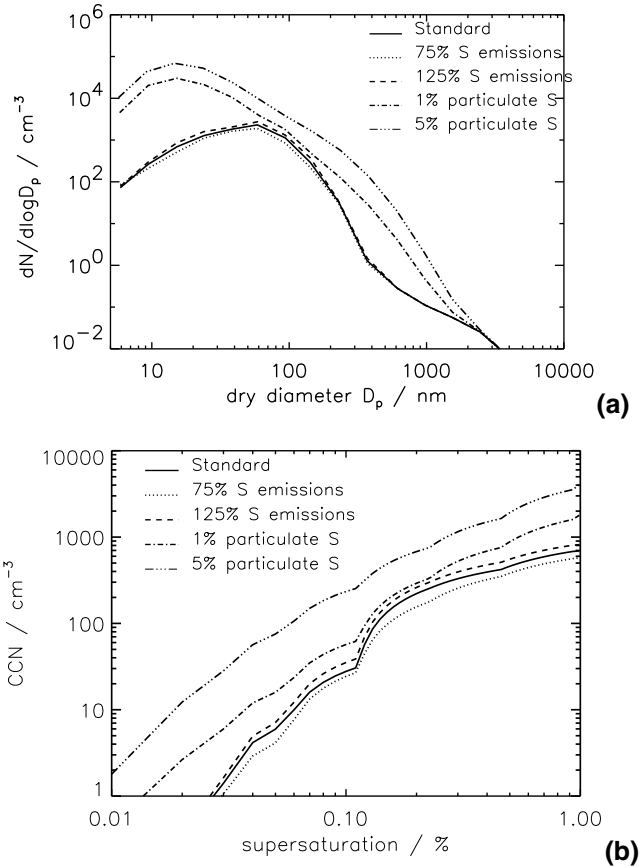

Fig. 16. Simulated monthly averaged BL (bottom model level) aerosol distributions over Northern Europe (50–60° N, 10–20°E) for December 1995 for different sulfur emission rates and percentages of particulate emissions. The baseline model runhas 100% sulfur emissions and 0% of the sulfur emissions emitted as particulates. **(a)** Number-size distribution; **(b)** CCN spectrum.

ACPD
5, 3437–3489, 2005

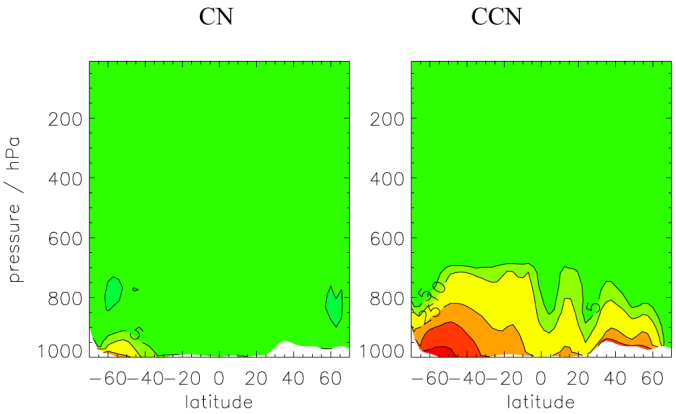

Fig. 17. Monthly mean change in zonal mean CN (% change) and CCN (absolute change (cm^{-3}) at 0.2% supersaturation) concentrations for December 1995 for sea salt emissions an order of magnitude higher than in the baseline case.

ACPD
5, 3437–3489, 2005

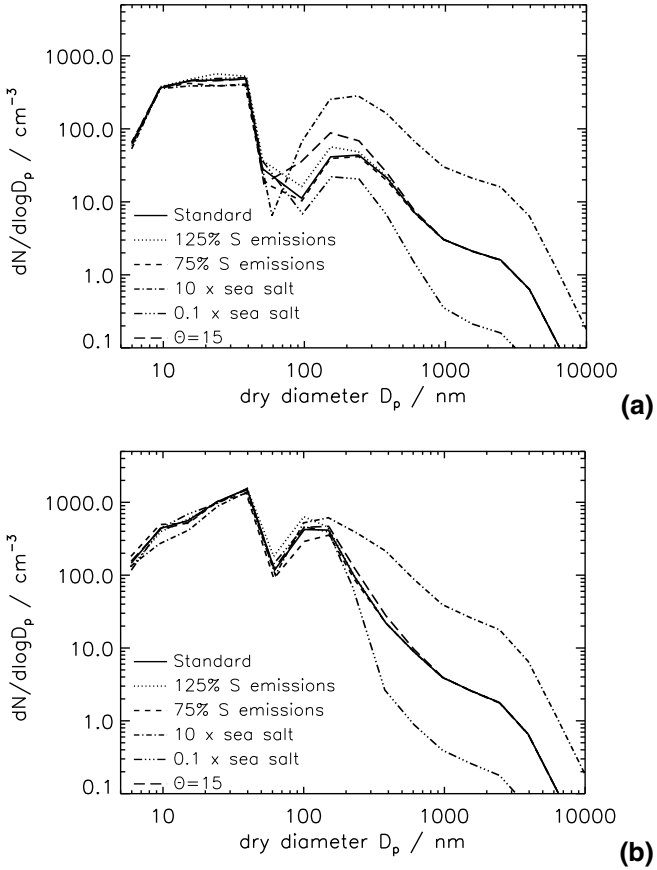

Fig. 18. Simulated monthly averaged MBL number-size distributions (bottom model level) for December 1995 over **(a)** Southern Ocean (50–55°S, 150–155° E); **(b)** North Atlantic (40–45° N, 30–35° W) for different sulfur and sea spray emission rates.

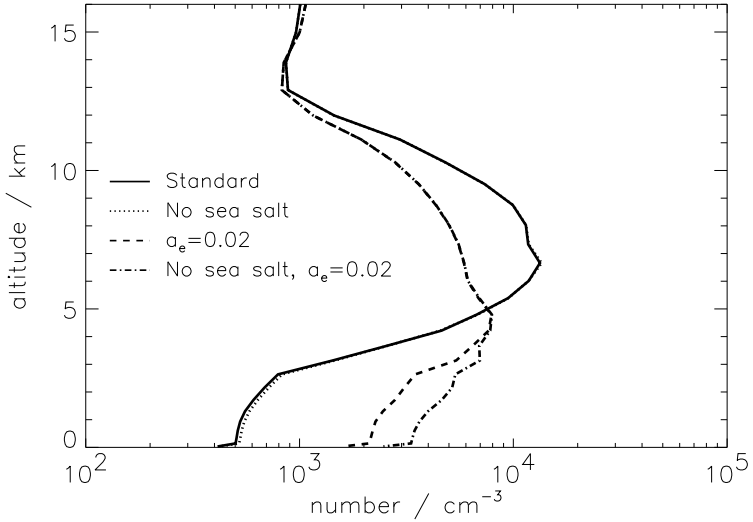

Fig. 19. Simulated monthly mean vertical profile of CN concentrations at STP in the Southern Ocean (50–55°S, 150–155° E) during December 1995 for different accommodation coefficients and sea spray emissions.

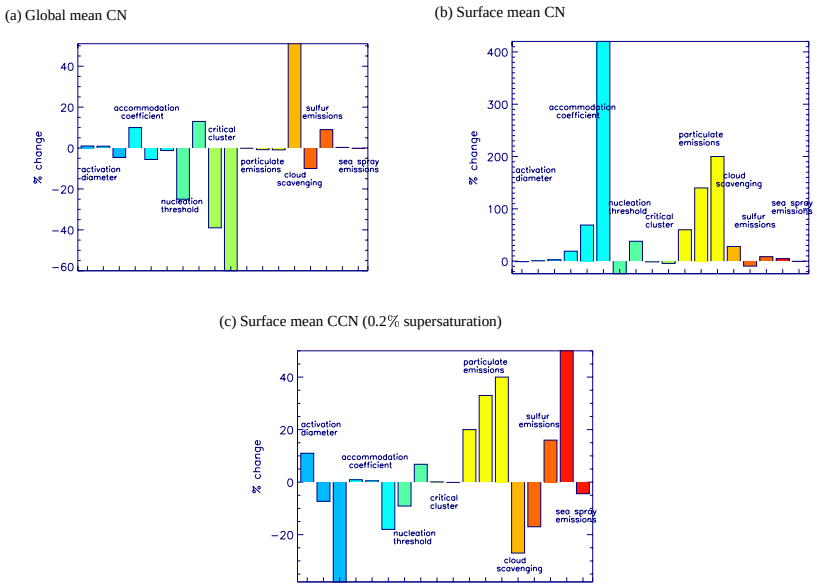

Fig. 20. Percentage change in monthly mean **(a)** Global mean CN, **(b)** surface mean CN, **(c)** surface mean CCN (at 0.2% supersaturation) during December 1995 for changes in model parameters. The model parameters were varied (left to right in the above panels) as follows: aqueous phase activation diameter – 0.04, 0.06, 0.08 μm (baseline model run 0.05 μm), accommodation coefficient – 0.02, 0.3, 0.65 (baseline 1.0), H_2SO_4 nucleation threshold 2 and 0.5 times the baseline; nucleation critical cluster size – 50 and 10 molecules (baseline 100 molecules H_2SO_4), particulate emissions – 1, 3 and 5% of anthropogenic SO_2 (baseline 0%), cloud scavenging activation diameter – 0.1 μm (baseline 0.206 μm), sulfur emissions – 75% and 125% of the baseline, sea spray emissions – 10 and 0.1 times the baseline flux.